Third International Conference on CFD in the Minerals and Process Industries
CSIRO, Melbourne, Australia
10-12 December 2003

CFD INVESTIGATION OF PARTICLE DEPOSITION AND DISTRIBUTION IN A HORIZONTAL PIPE

By Alamgir HOSSAIN[1], Jamal NASER[1], Kerry McMANUS[1], and Greg RYAN[2]

[1]School of Engineering and Science, Swinburne University of Technology, VIC 3122, AUSTRALIA
[2]South East Water Ltd, Moorabbin, VIC 3189, AUSTRALIA

ABSTRACT

Particle deposition and suspension in a horizontal pipe flow have been studied. A 3D numerical multiphase mixture model available in Fluent 6.0 is used. The model solves continuity and momentum equations for the mixture and volume fraction equations for the secondary phases. Transport equations were also solved for turbulence parameters of the particulate phases. Gravitational and hydrodynamic drag forces were included. The deposition was studied as a function of particle diameter, density and velocity of fluid. The deposition of particles, along the periphery of the wall, at different depths was also investigated. The deposition of heavier particles at the bottom of the pipe wall was found to be higher at lower velocities and lower at higher velocities. The lighter particles were found to remain mostly suspended with homogeneous distribution. Smaller particles also remained suspended with marginal higher concentration near the bottom of the wall. This marginal higher concentration of the smaller particles was found to be slightly pronounced for lower velocity. The larger particles clearly showed deposition near the bottom of the wall. This deposition was found to be pronounced at higher velocity.

NOMENCLATURE

$\vec{a}$	Acceleration (ms^{-2})
$\vec{v}_m$	Mass-averaged velocity (ms^{-1})
v	Free-flight velocity (ms^{-1})
v_g	Gravitational settling velocity (ms^{-1})
α_k	Particle Volume fraction
μ_m	Dynamic mixture viscosity (Pa-s)
ρ_m	Mixture density (kgm^{-3})
τ_{qp}	Particle Relaxation time (s)

INTRODUCTION

The importance of particle dispersion and deposition in two-phase flows has been well recognized in numerous different fields of research and industry. Some examples are the transport of pollutants in the atmosphere and oceans, droplets in sprays and internal combustion engines, slurries in pipes, sediment transport in coastal areas, catalyst particles in riser flows, particles deposition in annular dispersed two-phase flow, fluidized beds, dust deposition and dust removal in clean rooms, etc. In most applications one is interested in how particles are transported by turbulent flows and where the particles eventually end up.

The motivation for this study is two-fold, first we are interested in the deposition of solid spherical particles with specific gravity 3.0 as it occurs in annular dispersed two phase flows in water supply network. The dispersed phase of such flows consist of particles with diameters ranging from 5 μm to approximately 100 μm. This study was conducted for five different particle densities ranging from specific gravity (sg) 1.5 to approximately 6.0 keeping the diameter same at 10 μm. These flows are rather complex and it is difficult to obtain detailed experimental data on the contribution to deposition in relation to particle size. In order to obtain more insight into the process of particle deposition numerical simulations were carried out at different Reynolds numbers.

The second point of interest of this study is to investigate the segregation of solid particles along the circumference of the pipe wall. The Eulerian description of turbulence and the role of turbulent structures in the dispersion of particles give us a better understanding in the relationship between temporal and spatial properties of turbulent flows. When faced with the task of modeling turbulent particles deposition, or any multiphase flow, two general approaches are possible. One is Lagrangian approach, usually known as a "trajectory model" (Kallio and Reeks, 1989), where the instantaneous motions of individual particles are tracked by solving their equations of motion. The trajectories of many particles (typically thousands) are realised in order to form the average behavior of the particle-fluid system. The other is Eulerian, often called a "two-fluid" model, where the particles are treated as a continuous phase, in much the same way that a tracer fluid would be regarded in a binary mixture. The motion of the particulate phase is mathematically described by mass, momentum and energy conservation, similar to a fluid. In this study we followed Eulerian approach. In order to study the behavior of particles in a turbulent flow field numerically, one needs a proper representation of turbulence itself

The use of a horizontal cylindrical pipe (dia D = 472 mm and 330.4 m long) in combination with a large range of particle sizes and densities makes this study of relevance for many practical applications and makes a comparison with the numerous experiments on particle deposition possible.

GOVERNING EQUATION

The Multiphase Mixture Model (Spalart and Allmaras, 1992) of FLUENT 6.0 used in this study solves the

continuity and the momentum equation for the mixture. Volume fraction equations are solved for the secondary phases. The model also solves for the well-known algebraic expressions for the relative velocities for secondary phases (FLUENT 6.0 Manual, Chapter 20)

Continuity Equation for the Mixture

The continuity equation for the mixture is

$$\frac{\partial}{\partial t}(\rho_m) + \nabla \cdot (\rho_m \vec{v}_m) = 0 \quad (1)$$

where $\vec{v}_m$ is the mass-averaged velocity:

$$\vec{v}_m = \frac{\sum_{k=1}^{n} \alpha_k \rho_k \vec{v}_k}{\rho_m} \quad (2)$$

and ρ_m is the mixture density:

$$\rho_m = \sum_{k=1}^{n} \alpha_k \rho_k \quad (3)$$

α_k is the volume fraction of phase k.

Momentum Equation for the Mixture

The momentum equation for the mixture can be obtained by summing the individual momentum equations for all phases. It can be expressed as:

$$\frac{\partial}{\partial t}(\rho_m \vec{v}_m) + \nabla \cdot (\rho_m \vec{v}_m \vec{v}_m) = -\nabla p + \nabla \cdot \left[\mu_m \left(\nabla \vec{v}_m + \nabla \vec{v}_m^T\right)\right] + \rho_m \vec{g} + \vec{F} + \nabla \cdot \left(\sum_{k=1}^{n} \alpha_k \rho_k \vec{v}_{dr,k} \vec{v}_{dr,k}\right) \quad (4)$$

where n is the number of phases, $\vec{F}$ is a body force, and μ_m is the viscosity of the mixture:

$$\mu_m = \sum_{k=1}^{n} \alpha_k \mu_k \quad (5)$$

$\vec{v}_{dr,k}$ is the drift velocity for secondary phase k:

$$\vec{v}_{dr,k} = \vec{v}_k - \vec{v}_m \quad (6)$$

Relative (Slip) Velocity and the Drift Velocity

The relative velocity (also referred to as the slip velocity) is defined as the velocity of a secondary phase (p) relative to the velocity of the primary phase (q):

$$\vec{v}_{qp} = \vec{v}_p - \vec{v}_q \quad (7)$$

The drift velocity and the relative velocity ($\vec{v}_{qp}$) are connected by the following expression:

$$\vec{v}_{dr,p} = \vec{v}_{qp} - \sum_{k=1}^{n} \frac{\alpha_k \rho_k}{\rho_m} \vec{v}_{qk} \quad (8)$$

The basic assumption of the algebraic slip mixture model is that, to prescribe an algebraic relation for the relative velocity, a local equilibrium between the phases should be reached over short spatial length scales. The form of the relative velocity is given by

$$\vec{v}_{qp} = \tau_{qp} \vec{a} \quad (9)$$

where $\vec{a}$ is the secondary-phase particle's acceleration and τ_{qp} is the particulate relaxation time. Following Manninen et al. (1996) τ_{qp} is of the form:

$$\tau_{qp} = \frac{(\rho_m - \rho_p) d_p^2}{18 \mu_q f_{drag}} \quad (10)$$

where d_p is the diameter of the particles of secondary phase p, and the drag function f_{drag} is taken from Schiller and Naumann (1935):

$$f_{drag} = \begin{cases} 1 + 0.15 \mathrm{Re}^{0.687} & \mathrm{Re} \le 1000 \\ 0.0183 \mathrm{Re} & \mathrm{Re} > 1000 \end{cases} \quad (11)$$

and the acceleration $\vec{a}$ is of the form

$$\vec{a} = \vec{g} - (\vec{v}_m \cdot \nabla)\vec{v}_m - \frac{\partial \vec{v}_m}{\partial t} \quad (12)$$

The simplest algebraic slip formulation is the so-called drift flux model, in which the acceleration of the particle is given by gravity and/or a centrifugal force and the particulate relaxation time is modified to take into account the presence of other particles.

Volume Fraction Equation for the Secondary Phases

From the continuity equation for secondary phase p, the volume fraction equation for secondary phase p can be obtained:

$$\frac{\partial}{\partial t}(\alpha_p \rho_p) + \nabla \cdot (\alpha_p \rho_p \vec{v}_m) = -\nabla \cdot (\alpha_p \rho_p \vec{v}_{dr,p}) \quad (13)$$

RESULTS AND DISCUSSION

Figures 1 and 2 show the relative concentration (ratio of local concentration to bottom wall concentration) plotted as a function of particle diameter for different height of 0.25D, 0.5D, 0.75D, and 1D from the bottom wall of the pipe. Particles of size 5 μm are evenly distributed throughout the cross section of the pipe. The concentration of 10 μm size particles shows gradual increase towards the bottom. The concentration of 20 μm size particles is localized near the bottom. The larger size particles 50-100 μm are all localized at the bottom of the pipe.

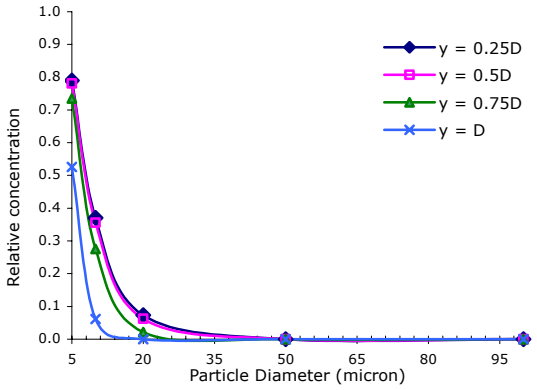

Figure 1: Relative concentration of particles for different height as a function of particle diameter for the velocity 0.1 ms^{-1}

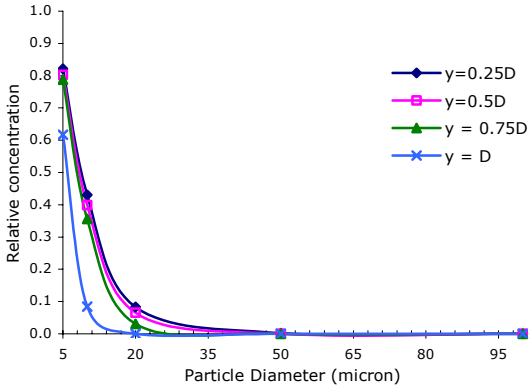

Figure 2: Relative concentration of particles for different height as a function of particle diameter for the velocity 0.5 ms^{-1}

This relative concentration distribution or the settling behavior discussed above (figures 1 and 2) can be explained by analyzing the settling velocity of the particle and the free flight velocity of the fluid. When the gravitational settling velocity of the particle, (Mols and Oliemans, 1996) is greater than the free flight velocity of the fluid (Binder and Hanratty, 1992) showed in tables 1 and 2, the particle tends to settle. This explains why the concentration of the larger particles is almost zero near the top wall. When the free-flight velocity is larger than the gravitational settling velocity, particles tends not to settle and can be seen dispersed in the cross section of the pipe (Kallio and Reeks, 1989; Mols and Oliemans, 1996). Tables 1 and 2 show that for diameters between 5 and 20 μm, particles have larger free flight velocities than its gravitational settling velocity so these particles tends not to settle and can be found at the top of the pipe as shown in figures 1 and 2.

Table 1: Free-flight velocity (v)

Fluid velocity	Free flight velocity
0.1 ms^{-1}	1.82×10^{-3} ms^{-1}
0.5 ms^{-1}	7.61×10^{-3} ms^{-1}

Table 2: Gravitational settling velocity (v_g) and its ratio to free-flight velocity (v)

Particle Size μm	Specific gravity	Settling velocity v_g ms^{-1}	Ratio = v_g/v at 0.1 ms^{-1}	Ratio = v_g/v at 0.5 ms^{-1}
5	3.0	4.09×10^{-05}	0.02	0.01
10		1.64×10^{-04}	0.09	0.02
20		6.54×10^{-04}	0.35	0.09
50		4.09×10^{-03}	2.21	0.55
100		1.64×10^{-02}	8.79	2.15
10	1.5	8.18×10^{-05}	0.04	0.01
	2.5	1.36×10^{-04}	0.07	0.02
	4.0	2.18×10^{-04}	0.12	0.03
	5.0	2.73×10^{-04}	0.15	0.04
	6.0	3.27×10^{-04}	0.20	0.05

The effect of flow velocity on the distribution particle concentration is shown in figure 3. The figure shows the relative concentration at top of the pipe (4.72×10^{-1} m) plotted as function of particle diameter. The distribution of the particles appears to be almost insensitive to the range of flow velocity investigated in this study.

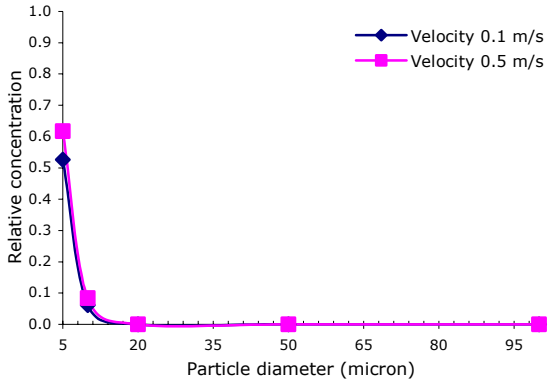

Figure 3: Comparison between the relative concentration of particles the top and the bottom of the channel as a function of particle diameter for the velocity 0.1 and 0.5 ms^{-1}

Local deposition rates along the pipe circumference can be obtained from the simulation. Figures 4-7 show typical circumferential distributions of particles volume fraction for various velocities. Most of the profiles exhibit a smooth variation with the maximum deposition at the bottom of the pipe. Similar trends were observed from the experimental data of Anderson & Russell (1970) and simulated results of Mols and Oliemans (1996).

Figures 4-5 show the volume fraction of different size particles (5, 10, 20, 50, and 100 μm, specific gravity 3.0) plotted as a function of the circumferential pipe angles. The angle 0^0 starts at the top wall and angle 180^0 is the bottom wall of the pipe. Particles ≥ 20 μm show greater concentration near the bottom wall of the pipe. The smaller size particles remain suspended and uniformly dispersed.

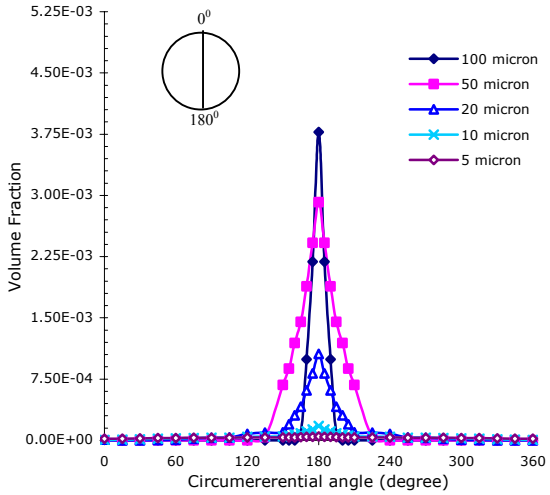

Figure 4: Circumferential deposition as a function of circumferential pipe angles for five different particle sizes for the velocity 0.1 ms^{-1}

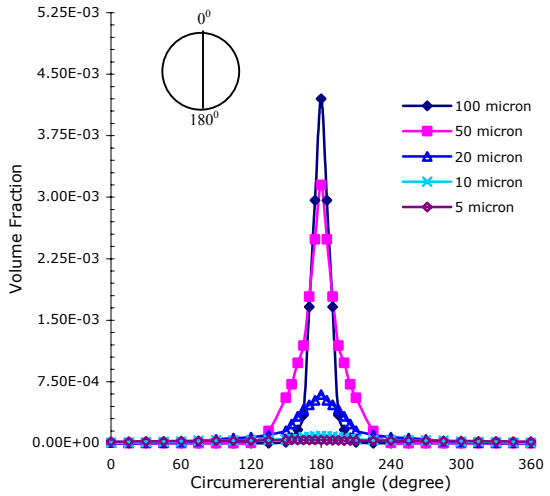

Figure 5: Circumferential deposition as a function of circumferential pipe angles for five different particle sizes for the velocity 0.5 ms^{-1}

The influence of the Reynolds number on the deposition on the pipe wall is also shown in the figures 4-5. Smaller the size of the particle, the larger the influence of the velocity change. This is an effect, which can be expected on the basis of the fact that for smaller particles the

influence of turbulent diffusion is relatively large in comparison with the influence of gravity. Therefore, the particles ≤ 20 μm have not been influenced by gravity and remained suspended. The uniformity of dispersion increases with the flow velocity. Larger particles, which are influenced by the gravity, settle more for higher velocity. This is because of resultant downward particle acceleration in equation (12) increases as the velocity increases; therefore, gravitational settling velocity increases [equation (9)].

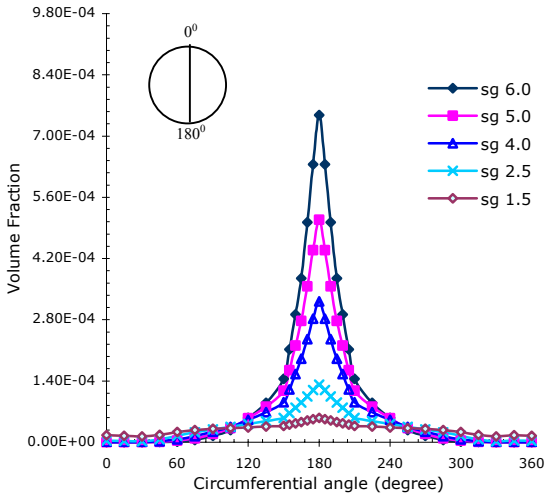

Figure 6: Circumferential deposition as a function of circumferential pipe angles for five different particle densities for the velocity 0.1 ms^{-1}

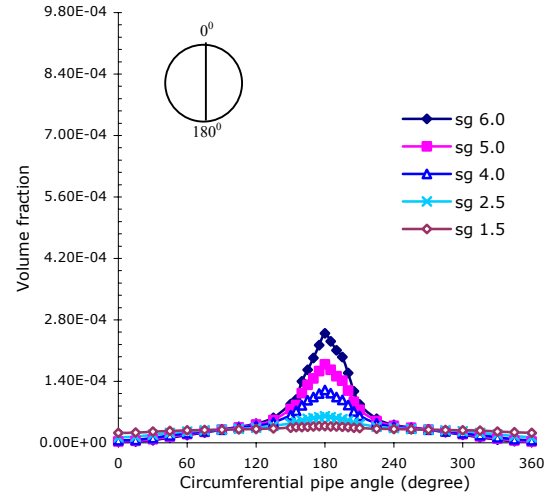

Figure 7: Circumferential deposition as a function of circumferential pipe angles for five different particle densities for the velocity 0.5 ms^{-1}

The influence of the Reynolds number on the deposition of 10 μm particle with different density is shown in the figures 6-7. These figures show the volume fraction of different density particles (1.5, 2.5, 4.0, 5.0, and 6.0 gm/cm^3, diameter 10 μm) plotted as a function of the circumferential pipe angles. The particles, which exhibit the ratio of settling velocity to free flight velocity (table 2) less than 0.5, are less sensitive to gravity force and strongly influenced by the diffusivity of the fluid, which increases due to increase of velocity (Mols and Oliemans, 1996). Table 2 shows that the ratio of free flight velocities to settling velocity for 0.1 ms^{-1} is relatively higher than that for 0.5 ms^{-1}. This resulted in higher concentration of heavier particles near the bottom of the pipe for lower velocity 0.1 ms^{-1} (figure 6) as compared to that of 0.5 ms^{-1} (figure 7).

CONCLUSION

This paper investigated the effect of particle size, particle density and Reynolds number on the deposition and dispersion in a horizontal pipe. The larger particles, which exhibit the ratio of gravitational settling velocity to free flight velocity (table 2) more than 0.5, in general, are influenced by gravity, and show a tendency of settlement. But smaller particles, which exhibit the ratio of gravitational settling velocity to free flight velocity, less than 0.5, are influenced by turbulent diffusivity and are dispersed more or less uniformly across the cross section of the pipe.

REFFERENCES

ANDERSON, R. J. and RUSSELL, T. W. F., (1970) "Film formation in two-phase annular flow." *AIChE Jl,* Vol 14, pp. 626-633.

BINDER, J. L. and HANRATTY, T. J., (1992), "Use of Lagrangian methord to describe drop deposition and distributio in horizontal gas-liquid annular flows." *Int. J. Multiphase Flow,* Vol 18. pp. 403-419.

HINZE, J. O., (1975), "Turbulence, 2nd Edition." *McGraw-Hill.*

KALLIO, G. A. and REEKS, M. W., (1989), "A Numerical simulation of particle deposition in turbulent boundary layers." *Int. J. Multiphase Flow*, Vol. 15, No. 3, pp. 433-446.

MANNINEN, M., TAIVASSALO, V., and KALLIO, S., (1996). "On the mixture model for multiphase flow." *VTT Publications 288, Technical Research Centre of Finland.*

MOLS, B. and OLIEMANS, R. V. A., (1998), "A Turbulent diffusion model for particle dispersion and deposition in horizontal tube flow." *Int. J. Multiphase Flow*, Vol. 24, No. 1, pp. 55-75.

PARASH, S. V. and KARABELAS, A. J., (1991), "Droplet entrainment and deposition in horizontal annular flow", *Int. J. Multiphase Flow*, Vol. 17, No. 4, pp. 455-468.

REYNOLDS, A. J., (1974), "Turbulent Flows in Engineering." *John Wiley & Sons*.

SCHILLER, L and NAUMANN, Z., (1935) *Z.Ver. Deutsch. Ing.*, 77:318.

SPALART, P. and ALLMARAS, S., (1992) "A one-equation turbulence model for aerodynamic flows.", *American Institute of Aeronautics and Astronautics*, Technical Report AIAA-92-0439.

UIJTTEWAAL, W. S. J. and OLIEMANS, R. V. A., (1996), "Particle dispersion and deposition in direct numerical and large eddy simulations of vertical pipe flows." *Phys. Fluids*, **8** (10), pp. 2590-2604.